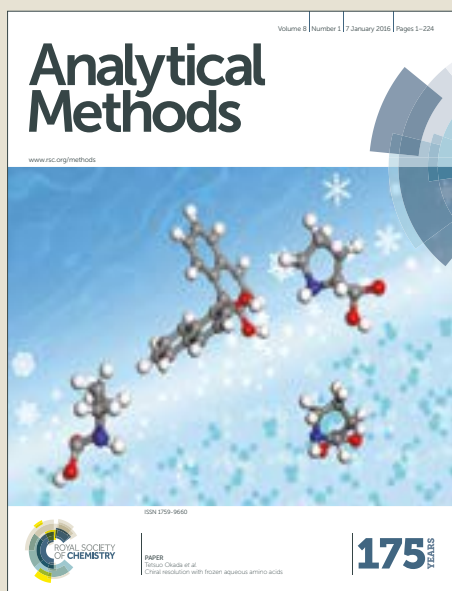


# Analytical Methods

Accepted Manuscript



This article can be cited before page numbers have been issued, to do this please use: E. Marin-Barroso, G. A. Messina, F. A. Bertolino, J. Raba and S. V. Pereira, *Anal. Methods*, 2019, DOI: 10.1039/C9AY00255C.



This is an Accepted Manuscript, which has been through the Royal Society of Chemistry peer review process and has been accepted for publication.

Accepted Manuscripts are published online shortly after acceptance, before technical editing, formatting and proof reading. Using this free service, authors can make their results available to the community, in citable form, before we publish the edited article. We will replace this Accepted Manuscript with the edited and formatted Advance Article as soon as it is available.

You can find more information about Accepted Manuscripts in the [author guidelines](#).

Please note that technical editing may introduce minor changes to the text and/or graphics, which may alter content. The journal's standard [Terms & Conditions](#) and the ethical guidelines, outlined in our [author and reviewer resource centre](#), still apply. In no event shall the Royal Society of Chemistry be held responsible for any errors or omissions in this Accepted Manuscript or any consequences arising from the use of any information it contains.

1  
2  
3 1  
4  
5  
6 2  
7  
8  
9 3  
10  
11 4  
12  
13  
14 5  
15 ***Electrochemical immunosensor modified with carbon nanofibers***  
16 ***coupled to a paper platform for the determination of gliadins in food***  
17 ***samples***  
18  
19 7  
20  
21 8  
22  
23  
24 9  
25  
26  
27 10  
28  
29  
30  
31  
32  
33  
34  
35  
36  
37  
38

39 11 *Evelyn Marín -Barroso, Germán A. Messina, Franco A. Bertolino, Julio Raba, Sirley V.*

40 12 *Pereira \**

41 13  
42 14 INQUISAL, Departamento de Química, Facultad de Química, Bioquímica y Farmacia, Universidad Nacional  
43 15 de San Luis, Chacabuco 917, San Luis, Argentina.

44 16  
45 17 Author to whom correspondence should be addressed: (e-mail) spereira@unsl.edu.ar. (Tel.)  
46 18 +54-266-4425385; (Fax) +54-266-443-0224.

47 19 INQUISAL, Departamento de Química. Universidad Nacional de San Luis, CONICET.  
48 20 Chacabuco 917. D5700BWS. San Luis, Argentina.

## 22 Abstract

23 The gluten-free diet is a unique, effective treatment for different conditions related to  
24 gluten consumption. Therefore, it is crucial the availability of new methodologies for the  
25 sensitive and specific determination of gluten content in food samples.

26 Herein, a screen printed electrode modified with carbon nanofibers coupled to a paper  
27 immunoaffinity platform was reported for the determination of gliadin in foods samples. The  
28 paper microzone covalently functionalized with specific anti-gliadin antibodies was placed  
29 on the modified electrode surface for the electrochemical determination of gliadin. The  
30 surface of the electrode modified with carbon nanofibers was characterized by scanning  
31 electron microscopy (SEM) and cyclic voltammetry (CV), which showed the improved  
32 sensitivity of the modified surface. The developed device was evaluated using different flour  
33 samples obtaining a favorable response. The calculated limit of detection for the device in  
34 analyzed samples was  $0.005 \text{ mg kg}^{-1}$  and for the Enzyme-linked immunosorbent assay was  
35  $1.5 \text{ mg kg}^{-1}$ . The coefficient of variation (CV) for the determination of  $20 \mu\text{g kg}^{-1}$  of gliadin  
36 was 4.11 %.

37 The disposable electrochemical sensor developed, represents an easy-to-use and low-  
38 cost strategy for the determination of gliadin in food samples.

39  
40 **Keyword: gliadin, immunosensor, electrochemistry, carbon nanofiber, food**

## 42 Introduction

43 The restriction of the consumption of foods containing gluten is the appropriate  
44 treatment for two different disorders, one of them is celiac disease, and the other is non-celiac  
45 gluten sensitivity. Celiac disease is an autoimmune enteropathy caused by exposure to food  
46 containing gluten in genetically susceptible individuals <sup>1</sup>. The prevalence of this pathology  
47 is 1% of the world's population <sup>2</sup>. This enteropathy generates chronic inflammation in the  
48 small intestine with villous atrophy and therefore malabsorption syndrome. Although some  
49 patients could be asymptomatic <sup>3,4</sup>, the frequent exposure to gluten cause symptoms as  
50 anemia, malnutrition, and alteration in growth. This disease can lead to significant  
51 complications as intestinal T-cell lymphoma and adenocarcinoma of the small intestine <sup>5</sup>.

52 On the other hand, studies on non-celiac gluten sensitivity began in the early 1980s.  
53 Currently, the number of patients diagnosed with this condition is increasing. Its diagnosis is  
54 based on the exclusion of celiac disease and wheat allergy, due to the superposition of  
55 symptomatology among these. Compared with the above mentioned conditions, non-celiac  
56 gluten sensitivity is characterized by a negative result of the anti-transglutaminase antibody,  
57 and a standard IgE value, respectively. The absence of an accurate diagnostic form makes  
58 difficult the determination of the prevalence. Although, it is estimated that it is higher than  
59 for celiac disease <sup>6</sup>.

60 Gluten proteins involved in the pathogenesis of this disease are contained in wheat,  
61 barley and rye grains. It is a complex protein, composed of two primary proteins: gliadins  
62 and glutenins contained in the endosperm of the seeds <sup>7</sup>. They are alcohol-soluble monomeric  
63 proteins, characterized by repetitive domains of proline and glutamine (prolamins). These  
64 amino acids cannot be degraded by pancreatic, gastric and intestinal enzymes, remaining in

65 the intestinal lumen through the edge of the brush of the small intestine, which causes the  
66 inflammatory response <sup>8-10</sup>.

67 As of today, the only way to manage celiac disease is the strict dietary abstinence  
68 from foods containing gluten<sup>11</sup>. Following this diet is difficult for celiac patients, due to  
69 variations in food labeling, misinformation, and cross-contamination <sup>12</sup>.

70 According to the *Codex Alimentarius*, the products considered as free from gluten are  
71 those that do not exceed 20 mg kg<sup>-1</sup> (20 ppm). Besides, it defines the concentrations that can  
72 contain foods labeled "reduced in gluten," between 20 mg kg<sup>-1</sup> y 100 mg kg<sup>-1</sup> <sup>13</sup>.  
73 Consequently, it is relevant to develop a sensitive and specific method to quantify gluten  
74 through detection of gliadin residues in food intended to celiac patients. The conversion  
75 factor prolamine/gluten widely used is 2, but the gluten composition can be affected by  
76 several parameters: botanical origin (*Triticum aestivum*, *Triticum aethiopicum*, *Triticum*  
77 *durum*) agricultural conditions and others <sup>14</sup>.

78 Common methods currently used for the detection of gluten content in foods are based  
79 on a sandwich or competitive enzyme-linked immune assay for gliadin <sup>15,16</sup> and wheat DNA  
80 recognition by polymerase chain reaction. These techniques present high sensitivity and  
81 specificity but require trained personnel, long incubation times and washing periods. For  
82 these reasons, it is crucial the availability of a fast, sensitive method to facilitate gluten  
83 detection, proper labeling and safe feeding for patients suffering from these conditions.

84 The paper matrix has been adopted as an attractive reaction and detection platform  
85 due to the following advantages: low cost, flexibility, biodegradability, porous permeability,  
86 and accessibility. The excellent chemical compatibility makes it a material extensively used  
87 in analytical and clinical chemistry <sup>17,18</sup>. The paper platforms are manufactured by modeling  
88 sheets of paper in a hydrophilic zone surrounded by hydrophobic barriers. Various techniques

1  
2  
3 89 are used for this purpose, for example, wax printing, photolithography, polydimethylsiloxane  
4  
5 90 printing (PDMS) and plasma treatment <sup>19,20</sup>. Wax printing is a quick and straightforward  
6  
7 91 technique, carried out by printing wax patterns on the paper surface for the formation of  
8  
9 92 hydrophobic barriers. Compared to other modeling techniques, this is inexpensive and  
10  
11 93 suitable for producing a significant quantity of wax printed papers <sup>21</sup>.

12  
13  
14 94 Recently, many efforts have been directed to combine different detection systems  
15  
16 95 with paper platforms. Electrochemistry is widely used for this purpose due to its advantages  
17  
18 96 like low cost, portability, high ability to detect low level concentrations and the possibility  
19  
20 97 of miniaturization <sup>22</sup>. Electrochemistry offers the option to use different detection platforms  
21  
22 98 as screen printed carbon electrodes (SPCE) modified with carbon-based nanomaterials <sup>23,24</sup>.  
23  
24 99 CNFs present cylindrical shape characterized by different stacking arrangements of graphene  
25  
26 100 sheets. Its mechanical resistance, chemical stability, and electrical proprieties are similar to  
27  
28 101 the rest of carbon nanomaterials (single wall carbon nanotubes (SWCNT), multiwall carbon  
29  
30 102 nanotubes (MWCNT), graphene (G), graphene oxide (GO)). However, CNFs have  
31  
32 103 irregularities on their outer surfaces which significantly increase the efficiency of electron  
33  
34 104 transfer on the electrode surface <sup>25–29</sup>.

35  
36  
37  
38  
39 105 In this article, we developed an electrochemical disposable immunosensor to  
40  
41 106 determine the gliadin content in foods intended for celiac patients. It combines the use of an  
42  
43 107 SPCE modified with carbon CNFs with a paper immunorecognition support. The presence  
44  
45 108 of the CNFs on SPCE provides an increase of the active area improving the sensitivity of the  
46  
47 109 sensor. The paper platform represents a practical and efficient surface for the highly specific  
48  
49 110 biorecognition of gliadin proteins present in food samples. In this sense, the sensor  
50  
51 111 developed represents a promising resource to be applied for gluten detection in food  
52  
53 112 production and for the control of marketed gluten-free food.  
54  
55  
56  
57  
58  
59  
60

## 113 **Materials and methods**

### 114 **Reagents and solutions**

115 All reagents used were of analytical reagent grade. Anti-gliadin (wheat)  
116 monoclonal antibody produced in mouse (Santa Cruz Biotechnology). Anti-gliadin  
117 peroxidase conjugate antibody, gliadin, bovine serum albumin (BSA), carbon tetrachloride,  
118 carbon nanofiber (graphitized (iron free) composed of conical platelets, D x L 100 nm x 20-  
119 200  $\mu\text{m}$ ), catechol (Q) and Whatman paper # 1 qualitative filter paper were purchased from  
120 Sigma-Aldrich. All buffer solutions were prepared with Milli-Q water.

121 The enzyme immunoassay for gliadin quantitative determination: R7001  
122 RIDASCREEN<sup>®</sup> Gliadin, gliadin standard and the Set of 3 Gliadin Assay Controls  
123 RIDASCREEN<sup>®</sup> were purchased from R-Biopharm AG-Darmstadt Germany and was used  
124 according to the manufacturer's instructions.

### 125 **Instrumentation**

126 Electrochemical measurements were performed using BAS 100 B/W (Bioanalytical  
127 Analyzer Electrochemical System, West Lafayette, IN, USA). Cyclic voltammograms and  
128 amperograms were obtained using a screen printed carbon electrode (SPCE) Italsens IS-C  
129 by PalmSens.

130 The ultrasonic bath (testlab, Argentina) model TB02 was used to achieve CNFs  
131 dispersion.

132 All pH measurements were made with an Orion Research Inc. (Orion Research Inc.,  
133 Cambridge, MA, USA) Model EA 940 equipped with a glass combination electrode (Orion  
134 Research Inc.).

1  
2  
3 135 The morphology of nanofiber films on the surface of the working electrode was studied  
4  
5 136 by scanning electron microscopy LEO 1450VP (SEM). The paper microzones were printed  
6  
7  
8 137 with a Xerox ColorQube 8870 printer.  
9

10 138 **Preparation of carbon nanofiber dispersion and electrochemical reduction on SPCE**  
11  
12 139 **surface**  
13

14 140 CNFs were chemically oxidized with 6 M HNO<sub>3</sub>. This chemical agent generates  
15  
16 141 groups rich in oxygen at the CNFs surface, increasing the capacity of dispersion and  
17  
18 142 solubility of CNFs<sup>25</sup>. After that, were sonicated for 6 h, washed with bidistilled water until  
19  
20 143 pH 7 and dried in an oven at 60°C. 30 µg mL<sup>-1</sup> CNFs dispersion in carbon tetrachloride was  
21  
22 144 prepared and sonicated (50-60 Hz) for about 2 h. After that, 5 µL of this dispersion were  
23  
24 145 placed on SPCE surface (CNFs/SPCE) and dried at room temperature. The electrochemical  
25  
26 146 reduction of CNFs was carried out by applying a constant potential of -1.2 V for 800 s, in 0.5  
27  
28 147 M NaNO<sub>3</sub> at pH 4.  
29  
30  
31  
32

33 148 **Wax patterning and antibody immobilization**  
34

35 149 The wax patterns were printed on Whatman paper # 1 qualitative filter paper using a  
36  
37 150 Xerox ColorQube 8870 printer. Previously, a 6 mm diameter microzone was designed with  
38  
39 151 Corel Draw 9.  
40

41  
42 152 The paper surface offers hydroxyl groups for bioconjugation process, but in pure  
43  
44 153 cellulose, they are unreactive<sup>30</sup>. For this reason, it is necessary an activation procedure by  
45  
46 154 plasma oxidation which allows the covalent bonding of antibodies on the paper cellulose  
47  
48 155 surface. The plasma treatment induces the rupture of the union between C3 and C4 of the  
49  
50 156 pyranose ring, forming a carbon radical and oxygen radical. Both radicals combine for the  
51  
52 157 formation of aldehyde groups. These aldehyde groups which form Schiff bases with the  
53  
54 158 amino groups of the antibodies.<sup>31</sup> Firstly, the paper was treated for 2 min by oxygen plasma  
55  
56  
57  
58  
59  
60

1  
2  
3 159 whose excitation frequency and power were 100 W and 13.56 MHz respectively. Secondly,  
4  
5 160 5  $\mu\text{L}$  of anti-gliadin antibodies solution of  $10 \mu\text{g mL}^{-1}$  were added to the paper surface and  
6  
7 161 incubated in a humid chamber for 30 min. Finally, it was washed with PBS buffer pH 7.2.  
8  
9

10 162 The modified paper surface obtained represents a practical and versatile platform  
11  
12 163 to perform the immunorecognition process before the electrochemical determination.  
13  
14

### 164 **Gliadin content determination**

15 165 The processed samples were common wheat flour, gluten-free flour, manioc flour,  
16  
17 166 rice flour and control flour samples of known concentrations of gliadin. The extraction  
18  
19 167 process was carried out with 60% ethanol because the used samples (flours) are raw  
20  
21 168 materials. In the case of foods samples exposed to enzymatic degradation, heat treatments,  
22  
23 169 mechanical and chemical processes, the use of a specific extraction solution is required  
24  
25 170 (Mendez Cocktail extraction solution – R-Biopharm, Germany).  
26  
27

28 171 In the first case, the gluten extraction was as follows: 0.3 g of each sample was  
29  
30 172 weighed and mixed with 3 mL of 60% ethanol. After that, the mixture was incubated at room  
31  
32 173 temperature for 30 min under continuous stirring. Finally, it was centrifuged at 8000 rpm for  
33  
34 174 10 min. The gliadin concentrations were determined in the obtained supernatants diluted  
35  
36 175 1:50. Following the procedure described above, the resulting dilution factor was 500.  
37  
38

39 176 The gliadin content determination using the functionalized paper platform and the  
40  
41 177 modified electrode was achieved with the following stages (Figure 1).  
42  
43

44 178 The functionalized paper support was subjected to a blocking procedure with BSA  
45  
46 179 1%, incubated in a humid chamber for 5 min and washed with buffer PBS. In the next step,  
47  
48 180 5  $\mu\text{L}$  of the samples were added in the microzone and incubated in the same conditions for  
49  
50 181 10 min. The functionalized paper platform was washed with PBS buffer pH 7.2. After that,  
51  
52  
53  
54  
55  
56  
57  
58  
59  
60

182 5  $\mu\text{L}$  of anti-gliadin antibody conjugate with HRP were added, incubated in a humid chamber  
183 for 5 min and washed with PBS buffer pH 7.2. (Table 1, Electronic supplementary Data A)

184 Finally, the paper platform was placed on the CNFs/SPCE surface for the gliadin  
185 electrochemical determination. To perform amperometric measurements the paper platform  
186 was exposed to the addition of 5  $\mu\text{L}$  of a 1 mM citrate-phosphate buffer solution pH 5  
187 applying a detection potential of - 0.15 V. Once the background current stabilized (20 s  
188 approximately), 5  $\mu\text{L}$  of a revealing solution containing 1 mM Q and 1 mM  $\text{H}_2\text{O}_2$  were  
189 incorporated. The beginning of the enzymatic product reduction could be observed at 25 s.  
190 Finally, the reduction current of o- benzoquinone (BQ) was measured at 60 s.

191 A dilution factor of 500 must further multiply the gliadin concentration values ( $\mu\text{g}$   
192  $\text{kg}^{-1}$  (ppb)) obtained from the calibration curve. Considering that gliadin usually represents  
193 50 % of the proteins present in gluten, this result should be multiplied by 2 to get the gluten  
194 concentration.

## 195 **Results and discussion**

### 196 **Modified electrode characterization**

197 In this work, we use CNFs as a nanomaterial for the modification of the SPCE surface.  
198 The CNFs/SPCE was also electrochemically characterized by CV of 1mM ferri/ferrocyanide  
199 redox couple ( $[\text{Fe}(\text{CN})_6]^{4-/3-}$ ) in PBS, pH 7.2. The potential scan was ranged from -0.15 to  
200 0.8 V at a scan rate of 0.075  $\text{V s}^{-1}$ . Figure 2 (a) shows the voltammograms corresponding to  
201 a blank signal for CNFs/SPCE (green line), unmodified (black line) and modified SPCE (red  
202 line). In this figure, it can be observed an improved peak current for CNFs/SPCE compared  
203 with unmodified SPCE, indicating that the incorporation of CNFs in the SPCE surface,  
204 improved the conductivity and increased the active surface area of the electrode.

Another electrochemical study of CNFs/SPCE was the effect of the scan rate on CVs (Figure 2b). As can be appreciated, the oxidation and reduction peak currents show a linear correlation with the square of scan rate (Figure 2b inset) in the evaluated range (0.02-0.3 V s<sup>-1</sup>). The obtained results expose the existence of a fast electrochemical and diffusion-controlled process. Figure 2(c) displays the evaluation of the ratio of the anodic and cathodic peak currents (I<sub>pa</sub>/I<sub>pc</sub>) as a function of the CNFs concentration. For this, we used 1mM [Fe(CN)<sub>6</sub>]<sup>4-/3-</sup> in PBS, pH 7.2. The electrochemical reversibility decay when the CNFs concentration is higher than 30 μg mL<sup>-1</sup>. Thus, 30 μg mL<sup>-1</sup> of a CNFs solution were used for electrode modification.

The proposed method employs an enzymatic mediator with electrochemical activity, which is incorporated into the developer solution. Therefore, it is necessary to evaluate the behavior of the same in the CNFs/SPCE surface by cyclic voltammetry. This study was performed with a solution of 1 mM Q in 1 mM citrate-phosphate buffer pH 5 in the same experimental condition described for the obtaining of figure 2(a). The Figure 2 (d) shows the voltammograms corresponding to a blank signal for CNFs/SPCE (green line), unmodified (black line) and modified SPCE (red line). This cyclic voltammetry show one anodic and a corresponding cathodic peak which corresponds to the transformation of Q to BQ and vice-versa within a quasi-reversible two-electron process<sup>32</sup>. Likewise, to the figure 2 a, an improved peak current for CNFs/SPCE compared with unmodified SPCE was obtained. Additionally, the effect of the paper platform placed on the surface of the CNF / SPCE was evaluated. This comparative study revealed an insignificant variation in the obtained signals. (Electronic supplementary Data B).

1  
2  
3 227 To characterize the surface morphology of SPCE before and after of CNFs  
4  
5 228 incorporation, was carried out by scanning electron microscopy (SEM). Figure 3 (a) shows  
6  
7 229 the image of unmodified SPCE. Figure 3 (b) shows the image of CNFs/SPCE, which reveals  
8  
9 230 the adequate distribution of CNFs on the SPCE surface by generating a homogeneous CNFs  
10  
11 231 film with a compressed three-dimensional structure. The CNFs have an average diameter of  
12  
13 232 100 nm. These nanomaterials could be an excellent platform for electrochemical  
14  
15 233 transduction, as they significantly increase the active surface of the electrode. Besides, as  
16  
17 234 mentioned above, CNFs improve conductivity by providing a possible pathway for electron  
18  
19 235 transfer.

## 236 **Optimization**

### 237 **Electrode modification conditions**

238 Several variables were optimized to maximize the sensitivity of the proposed method.  
239 One of these was the optimum dispersion media of CNFs. This parameter was evaluated  
240 using 60  $\mu\text{g}$  of CNFs and 2 mL of methanol, dimethylformamide and carbon tetrachloride.  
241 A better dispersion media found was carbon tetrachloride. This dispersion was dropped on  
242 the SCPE and dried for 4 min at room temperature.

243 The CNFs electroreduction on the electrode surface is strongly affected by several  
244 parameters, such as the reduction time and reduction potential. Both factors have been  
245 optimized to obtain the best analytical performance. For the optimization of the reduction  
246 time the potential was set at -1.2 V and the reduction time was evaluated in a range of 100-  
247 900 s using 1mM  $[\text{Fe}(\text{CN})_6]^{4-/3-}$  in PBS, pH 7.2. As figure 3 (c) shows, the current grows with  
248 the increase of the reduction time until a value of 800 s, and then it remained constant.  
249 Therefore, a reduction time of 800 s was selected as optimum time. Regarding the reduction

potential, the time used was 800 s, and the working electrode potential was varied from -0.7 to -1.5 V in the experimental conditions described for electroreduction time optimization. As shown in Figure 3(d), the current increased slowly by increasing potential up to a value of -0.9 V, then grew rapidly from -0.9 to -1.2 V and remained constant from -1.2 to -1.4 V. Therefore, a reduction potential of -1.2 V was selected as optimum potential.

### Immunoassay optimization

The antibody concentration to be immobilized on the paper surface represents a relevant parameter to be optimized. Higher concentrations of antibodies cause adsorption in multiple layers, which would generate interference<sup>33</sup>. In our case, the optimum concentration of anti-gliadin antibody to be immobilized was evaluated by HRP saturation method. For this purpose, increasing antibody concentrations (1 - 14  $\mu\text{g mL}^{-1}$ ) were added in the paper microzone. Later, a constant and saturating amount of Horseradish peroxidase (HRP) (5 mg in 0.1 mL of PBS) was incorporated. HRP adsorbed in the available sites that were not previously occupied by antibodies. After that, paper microzones were placed on the electrode surface. The substrate solution containing 1 mM  $\text{H}_2\text{O}_2$  and 1 mM Q in 1 mM citrate-phosphate buffer pH 5 was added. HRP in the presence of  $\text{H}_2\text{O}_2$  catalyzes the oxidation of Q to BQ. The electrochemical reduction back to Q was detected on CNFs/SPCE at -0.15 V. As can be seen in fig.2(a) in electronic supplementary materials (C) the generated current reduces when antibody concentration increase, due to the lower availability of sites for HRP adsorption. Therefore, the generated current was inversely proportional to the amount of immobilized antibody. The optimum value of immobilized anti-gliadin antibodies was 10  $\mu\text{g mL}^{-1}$ .

1  
2  
3 272 Finally, the incubation time was evaluated due to it is an essential factor when the  
4  
5 273 reduction of the assay time is required. This parameter was evaluated using three different  
6  
7 274 standard concentrations. For low concentration standards, the signal growth with the increase  
8  
9 275 of gliadin concentration, while, for high concentration standard, the intensity of the current  
10  
11 276 increased until 10 min of incubation time due to saturation of the specific antibody binding  
12  
13 277 sites. Thus, the optimal reaction time was 10 min (Electronic supplementary Data C (b)).

### 278 **Analytical performance**

279 Gliadin quantitative detection in food samples was performed with the designed  
280 electrochemical immunosensor. A linear relation,  $i \text{ (nA)} = 2.7718 + 11.45 \times C \text{ gliadin}$  (figure  
281 4a), was observed between the current signal and the gliadin concentration in the range of 0  
282 and  $80 \mu\text{g kg}^{-1}$ . The correlation coefficient ( $r$ ) for this plot was 0.998. The coefficient of  
283 variation (CV) for the determination of  $20 \mu\text{g kg}^{-1}$  of gliadin was 4.11 % (six replicates).  
284 Furthermore, the limit of detection (LOD) for the electrochemical device in analyzed samples  
285 was  $0.005 \text{ mg kg}^{-1}$ , considering LOD as the concentration that gives a signal 3.29 times the  
286 standard deviation of the blank above its signal.

287 The accuracy of the electrochemical immunosensor was tested with a dilution test,  
288 which was performed with  $20 \mu\text{g kg}^{-1}$  gliadin standard concentration serially diluted in 0.01  
289 M PBS pH 7.2. (Electronic supplementary Data D).

290 ELISA procedure was also carried out. Absorbance changes were plotted against the  
291 corresponding gliadin concentration, and a calibration curve was constructed. The linear  
292 regression equation was  $A = 0.165 + 0.026 \times C_{\text{gliadina}}$  with the linear relation coefficient  $r^2 =$   
293 0.991, the CV for the determination of  $20 \mu\text{g kg}^{-1}$  of gliadin was 5.3 % (six replicates). For  
294 ELISA procedure, the LOD was  $1.5 \text{ mg kg}^{-1}$ .

1  
2  
3 295 The obtained gliadin concentration values for samples using the immunosensor were  
4  
5 296 compared with those obtained by the official Type I method for the determination of gliadin,  
6  
7 297 endorsed by the *Codex Alimentarius Commission* (ELISA R5 Méndez) as the official analysis  
8  
9 298 method for quality assessment of the gluten-free food. The slope obtained was reasonably  
10  
11 299 close to 1, indicating good correspondence between the two methods (Electronic  
12  
13 300 supplementary Data E). Compared with spectrophotometric ELISA method, the  
14  
15 301 immunosensor showed improved sensitivity, which allows the determination of very low  
16  
17 302 levels of gliadin and consequently the gluten content (Electronic supplementary Data F).

### 303 **Selectivity, reproducibility, and stability**

304 The selectivity, reproducibility, and stability are also critical analytical factors for  
305 gliadin determination. The selectivity of the system was investigated against the following  
306 reagents: albumin, casein, glutenin from wheat, gliadin,  $\beta$  lactoglobulin, and folic acid. The  
307 experiment was tested by the solutions with gliadin ( $40 \mu\text{g kg}^{-1}$ ) and different interference  
308 substances ( $40 \mu\text{g kg}^{-1}$ ). As figure 4(b) shows, only casein exhibited an increase of 39.9% in  
309 the analytical signal. This result represents a relevant data due to skin milk which contains  
310 casein is one of the agents widely used for blocking procedure. For this reason, BSA was  
311 selected as a blocking agent. This result is consistent with previously reported data <sup>34</sup>. The  
312 other agents displayed negligible signals. The results indicated the high selectivity of the  
313 sensor.

314 The precision of the disposable immunosensor was evaluated with intra and inter-  
315 assay approaches. These were performed by replicating the experiment six times using the  
316 immunofunctionalized paper microzone incorporated on CNFs-SPCE for each analyte  
317 concentration. The intra and inter-assay CV% obtained from six replicates using three

1  
2  
3 318 gliadin standard concentrations ( $5 \mu\text{g kg}^{-1}$ ,  $20 \mu\text{g kg}^{-1}$  and  $80 \mu\text{g kg}^{-1}$ ) were in a range of  
4  
5 319 3.87% and 6.56%, respectively (Electronic supplementary Data G). These results expose the  
6  
7  
8 320 satisfactory repeatability and reproducibility of the sensor.  
9

10  
11 321 The stability of the device was also evaluated. For this purpose, six lyophilized paper  
12  
13 322 microzones in PBS buffer pH 7 and six CNFs-SPCE were stored for three months at  $4^\circ\text{C}$ .  
14  
15 323 The devices showed the same currents as those used immediately after its design. The signals  
16  
17 324 were obtained in the same conditions described before for the flour samples.  
18  
19

### 20 325 **Real samples analysis**

21  
22 326 To demonstrate the applicability of the designed electrochemical device the gliadin  
23  
24 327 concentration was measured in 11 flour samples (manioc flour, rice flour, gluten-free flour,  
25  
26 328 and common wheat flour) and 3 control samples (Figure 4c). It is relevant to note that the  
27  
28 329 analyzed samples did not contain casein. The samples were spiked with a gliadin  
29  
30 330 concentration of  $10 \text{ mg kg}^{-1}$  after extraction procedure to obtain relative recovery. The gliadin  
31  
32 331 concentration values founded should be multiplied by a factor of 2<sup>35</sup>. The relative recoveries  
33  
34 332 of the spiked samples ranged from 98.50% to 102.10% with a CV fewer than 4.93%, which  
35  
36 333 showed an adequate accuracy for gliadin determination in food samples (Table 1).  
37  
38  
39

### 40 334 **Discussion**

41  
42 335 During the last 10 years, numerous studies describing different methodologies for the  
43  
44 336 determination of gliadins in food matrices have been published. Among them, it is essential  
45  
46 337 to mention commercial immunoassay kits which include multiple steps, long incubation  
47  
48 338 times and a large amount of reactive and samples<sup>33</sup>. Moreover, complex methods as LC-  
49  
50 339 MS/MS have been reported. This methodology represents a powerful tool, making possible  
51  
52 340 to detect individually wheat, oats, barley, and rye in a single chromatographic run. Although,  
53  
54  
55  
56  
57  
58  
59  
60

341 it requires trained personnel, expensive equipment and includes cumbersome sample  
342 pretreatment and time-consuming extraction and digestion steps<sup>36</sup>.

343 Nowadays, it relevant the availability of fast, sensitive and specific methodologies for  
344 routine control of gluten in food samples, providing the correct labeling for safe feeding. This  
345 requirement has generated an exponential grow of sensor technologies development. The  
346 bioanalytical sensor for gluten detection could be classified according to biorecognition agent  
347 employed. For gliadin detection immunosensors and aptasensors have been developed.  
348 Recently aptasensors coupled to electrochemical detection based on competitive format have  
349 been described <sup>37–39</sup>. These sensors allowed the determination of hydrolyzed and whole  
350 gluten with adequate LODs. However, the same articles have reported that the  
351 immobilization of aptamer generates a deleterious effect over its affinity, being more  
352 advantageous the attachment of the complementary peptide in the competitive assay.

353 Immunosensors with competitive and sandwich format couplet to different detection  
354 system have also been reported. The selection of the immunological model depends on the  
355 sample type. When samples contain whole gluten, the sandwich format and ELISA R5  
356 Méndez confirmation are adequate, while for samples with hydrolyzed gluten the competitive  
357 form represents the best choice. In this sense, several articles related to immunosensors  
358 designed have been reported. Electrochemical immunosensor using magnetic particles  
359 modified with the anti-gliadin antibody <sup>40</sup> was described. The use of these particles requires  
360 long incubation periods for the gliadin capture and detection. Microfluidic immunosensor  
361 with impedance spectroscopy was also described <sup>41</sup>. This device represents a portable tool  
362 which requires the use of different techniques and materials for the microfluidic platform

1  
2  
3 363 construction and pump system for the flow generation. Immunosensors can also be coupled  
4  
5 364 with a fluorescence detection system <sup>42</sup>, which offers is characteristic sensitivity.  
6  
7

8 365 The electrochemical device developed in this work is the only one based on the paper  
9  
10 366 support for the immunorecognition process. This platform of high availability, accessibility,  
11 367 and low cost was covalently functionalized with anti-gliadin antibodies. The analyzed  
12 368 samples contain whole gluten, being the sandwich type format the suitable for this  
13 369 application. The electrochemical detection was performed by SPCE modified with CNFs  
14 370 which allowed us to reach the less LOD compared to the described articles (Table 2). Finally,  
15 371 the proposed system requires an analysis time of 28 min, less than the compared methods.  
16  
17

## 372 **Conclusion**

18 373 In this work, a novel electrochemical disposable device was developed based on an  
19 374 innovative paper immunoaffinity reaction platform combined with the use of SPCE modified  
20 375 with CNFs as the detection system. The wax printing technique and plasma oxidation  
21 376 treatment allowed to obtain a delimited reaction area in the paper surface, where antibodies  
22 377 were covalently immobilized. This stable, specific and practical recognition platform was  
23 378 implemented to perform the gliadin determination by using a non competitive assay format  
24 379 in flour samples. The incorporation of CNFs allowed obtaining the increase of electron  
25 380 transfer efficiency and the active area enabling the determination of low levels of gliadin in  
26 381 food samples. Besides, the electrochemical detection can be done within 1 min and the  
27 382 complete assay in 28 min, much less than the reported methodologies. These features  
28 383 revealed the valuable contribution of this technology for gluten-free food control applications  
29 384 requiring a disposable device to perform fast, sensitive and selective determinations.  
30  
31  
32  
33  
34  
35  
36  
37  
38  
39  
40  
41  
42  
43  
44  
45  
46  
47  
48  
49  
50  
51  
52  
53  
54  
55  
56  
57  
58  
59  
60

## 385 Acknowledgements

386 Support from Universidad Nacional de San Luis (PROICO-1512-22/Q232), to the  
387 Agencia Nacional de Promoción Científica y Tecnológica (PICT-2013-2407. PICT-2013-  
388 3092, PICT-2014-1184, PICT-2015-1575, PICT-2015-2246) and from Consejo Nacional de  
389 Investigaciones Científicas y Técnicas (CONICET PIP-11220150100004CO) (Argentina)  
390 are acknowledged.

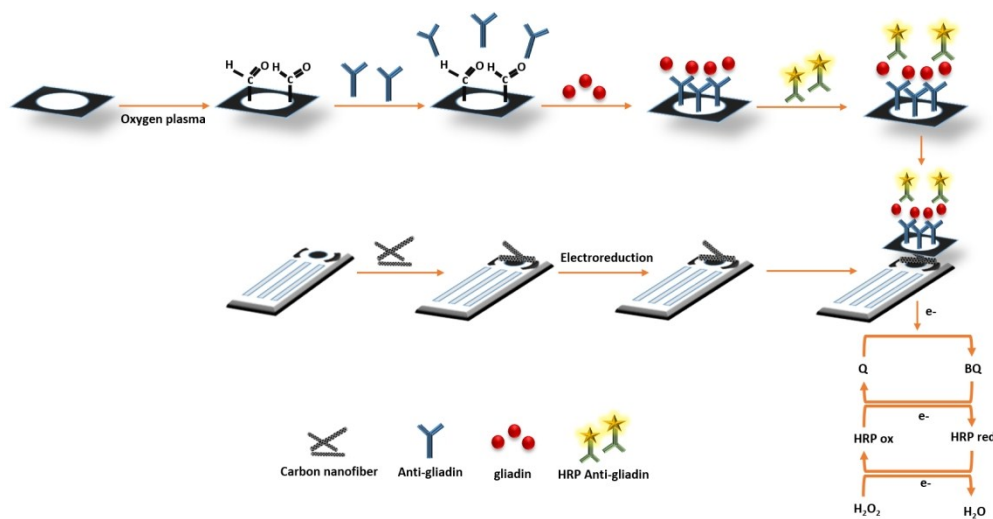
## 391 Reference

- 392 1 L. Shan, Ø. Molberg, I. Parrot, F. Hausch, F. Filiz, G. M. Gray, L. M. Sollid and C.  
393 Khosla, *Science* (80-. ), 2002, **297**, 2275–2279.
- 394 2 K. Barada, A. Bitar, M. A.-R. Mokadem, J. G. Hashash and P. Green, *World J.*  
395 *Gastroenterol.*, 2010, **16**, 1449–57.
- 396 3 E. Arranz and J. A. Garrote, *Gastroenterol. Hepatol.*, 2010, **33**, 643–651.
- 397 4 C. P. Kelly, J. C. Bai, E. Liu and D. A. Leffler, *Gastroenterology*, 2015, **148**, 1175–  
398 1186.
- 399 5 R. Baños Madrid, J. Mercader Martínez, F. Sánchez Bueno and A. Bas Bernal, *An.*  
400 *Med. Interna*, 2002, **19**, 81–84.
- 401 6 J. Molina-Infante, S. Santolaria, M. Montoro, M. Esteve and F. Fernandez-Banares,  
402 *Gastroenterol. Hepatol.*, 2014, **37**, 362–371.
- 403 7 Y. Van De Wal, Y. M. C. Kooy, P. Van Veelen, W. Vader, S. A. August, J. W.  
404 Drijfhout, S. A. Peña and F. Koning, *Eur. J. Immunol.*, 1999, **29**, 3133–3139.
- 405 8 M. Malalgoda and S. Simsek, *Food Hydrocoll.*, 2017, **68**, 108–113.
- 406 9 I. Polanco Allué and Isabel, *Enferm. celiaca y Sensib. al gluten no celiaca*, 2013, **0**,  
407 219–232.
- 408 10 I. Polanco Allué and C. Ribes Koninckx, *Protoc. diagnósticos- Ter. Gastroenterol.*

- 1  
2  
3 409 *Hepatol. y Nutr. pediátrica.*, 2010, **8**, 37–45.
- 4  
5 410 11 P. H. R. Green and C. Cellier, *n engl j med*, 2007, **357**, 1731–1743.
- 6  
7 411 12 B. Morón, M. T. Bethune, I. Comino, H. Manyani, M. Ferragud, M. C. López, Á.  
8  
9 Cebolla, C. Khosla and C. Sousa, *PLoS One*, , DOI:10.1371/journal.pone.0002294.
- 10  
11 412  
12 413 13 H. Yin, P. Chu, W. Tsai, H. W.-F. Chemistry and U. 2016, *Elsevier*, 2016, **192**, 934–  
13  
14 414 942.
- 15 415 14 K. L. Fiedler, S. C. McGrath, J. H. Callahan and M. M. Ross, *J. Agric. Food Chem.*,  
16  
17 416 2014, **62**, 5835–5844.
- 18 417 15 R. Haraszi, H. Chassaing, A. Maquet and F. Ulberth, *J. AOAC Int.*, 2011, 94, 1006–  
19  
20 418 1025.
- 21 419 16 T. Thompson and E. Méndez, *J. Am. Diet. Assoc.*, 2008, **108**, 1682–1687.
- 22 420 17 P. Andersson, D. Nilsson, P. O. Svensson, M. Chen, A. Malmström, T. Remonen, T.  
23  
24 421 Kugler and M. Berggren, *Adv. Mater.*, 2002, **14**, 1460–1464.
- 25 422 18 E. Fortunato, N. Correia, P. Barquinha, L. Pereira, G. Goncalves and R. Martins,  
26  
27 423 *IEEE Electron Device Lett.*, 2008, **29**, 988–990.
- 28 424 19 M. Ueland, L. Blanes, R. V. Taudte, B. H. Stuart, N. Cole, P. Willis, C. Roux and P.  
29  
30 425 Doble, *J. Chromatogr. A*, 2016, **1436**, 28–33.
- 31 426 20 W. Dungchai, O. Chailapakul and C. S. Henry, *Anal. Chem.*, 2009, **81**, 5821–5826.
- 32 427 21 E. Carrilho, A. W. Martinez and G. M. Whitesides, *Anal. Chem.*, 2009, **81**, 7091–  
33  
34 428 7095.
- 35 429 22 S. V. Pereira, J. Raba and G. A. Messina, *Anal. Bioanal. Chem.*, 2010, **396**, 2921–  
36  
37 430 2927.
- 38 431 23 J. Ezzati Nazhad Dolatabadi and M. De La Guardia, *Anal. Methods*, 2014.
- 39  
40 432 24 C. Pérez-Ràfols, N. Serrano, J. M. Díaz-Cruz, C. Ariño and M. Esteban, *Anal. Chim.*

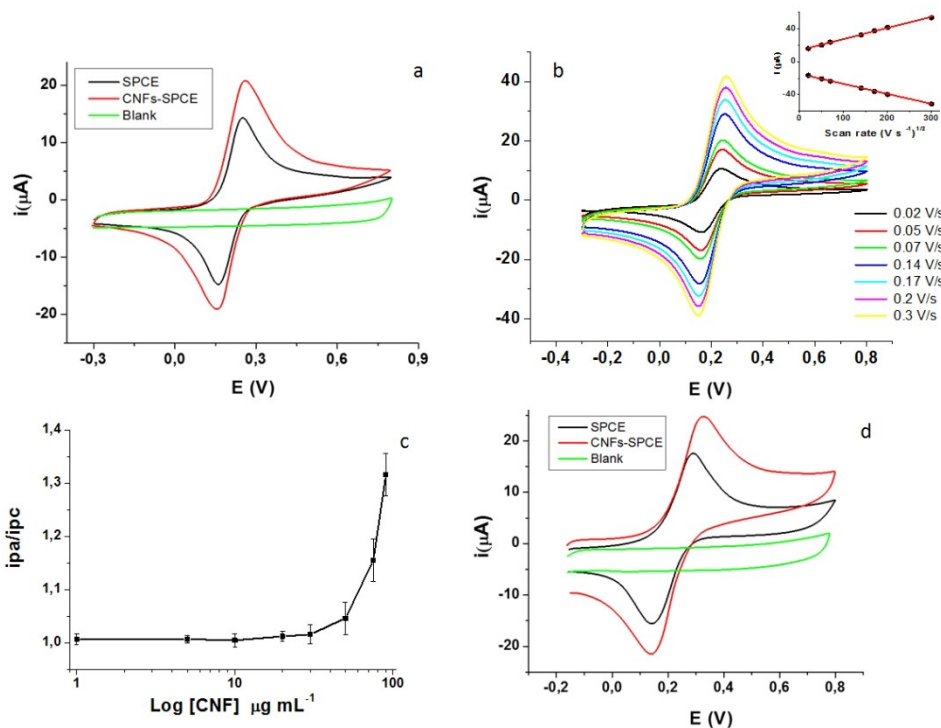
- 1  
2  
3 433 *Acta*, 2016, **916**, 17–23.
- 4  
5 434 25 J. Huang, Y. Liu and T. You, *Anal. Methods*, 2010, **2**, 202–211.
- 6  
7 435 26 B. Rezaei, M. Ghani, A. M. Shoushtari and M. Rabiee, *Biosens. Bioelectron.*, 2016,  
8  
9 436 78, 513–523.
- 10  
11 437 27 S. E. Baker, K.-Y. Tse, C.-S. Lee and R. J. Hamers, *Diam. Relat. Mater.*, 2006, **15**,  
12  
13 438 433–439.
- 14  
15 439 28 E. Rand, A. Periyakaruppan, Z. Tanaka, D. A. Zhang, M. P. Marsh, R. J. Andrews,  
16  
17 440 K. H. Lee, B. Chen, M. Meyyappan and J. E. Koehne, *Biosens. Bioelectron.*, 2013,  
18  
19 441 **42**, 434–438.
- 20  
21 442 29 S. Eissa, N. Alshehri, M. Abduljabbar, A. M. A. Rahman, M. Dasouki, I. Y. Nizami,  
22  
23 443 M. A. Al-Muhaizea and M. Zourob, *Biosens. Bioelectron.*, 2018, **117**, 84–90.
- 24  
25 444 30 L. Cao, C. Fang, R. Zeng, X. Zhao, Y. Jiang and Z. Chen, *Biosens. Bioelectron.*,  
26  
27 445 2017, **92**, 87–94.
- 28  
29 446 31 M. Zhao, H. Li, W. Liu, Y. Guo and W. Chu, *Biosens. Bioelectron.*, 2016, **79**, 581–  
30  
31 447 588.
- 32  
33 448 32 D. Nematollahi, M. Rafiee and A. Samadi-Maybodi, *Electrochim. Acta*, 2004, **49**,  
34  
35 449 2495–2502.
- 36  
37 450 33 N. Sajic, M. Oplatowska-Stachowiak, L. Streppel, J.-W. Drijfhout, M. Salden and F.  
38  
39 451 Koning, *Food Control*, 2017, **80**, 401–410.
- 40  
41 452 34 A. Vojdani and I. Tarash, *Food Nutr. Sci.*, 2013, **4**, 20–32.
- 42  
43 453 35 P. T. Chu and H. W. Wen, *Anal. Chim. Acta*, 2013, **787**, 246–253.
- 44  
45 454 36 A. Manfredi, M. Mattarozzi, M. Giannetto and M. Careri, *Anal. Chim. Acta*, 2015,  
46  
47 455 **895**, 62–70.
- 48  
49 456 37 L. López-López, R. Miranda-Castro, N. de-los-Santos-Álvarez, A. J. Miranda-

- 1  
2  
3 457 Ordieres and M. J. Lobo-Castañón, *Sensors Actuators, B Chem.*, 2017, **241**, 522–  
4  
5 458 527.  
6  
7  
8 459 38 F. Malvano, D. Albanese, R. Pilloton and M. Di Matteo, *Food Control*, 2017, **79**,  
9  
10 460 200–206.  
11  
12 461 39 S. Amaya-González, L. López-López, R. Miranda-Castro, N. de-los-Santos-Álvarez,  
13  
14 462 A. J. Miranda-Ordieres and M. J. Lobo-Castañón, *Anal. Chim. Acta*, 2015, **873**, 63–  
15  
16 463 70.  
17  
18 464 40 T. Laube, S. V. Kergaravat, S. N. Fabiano, S. R. Hernández, S. Alegret and M. I.  
19  
20 465 Pividori, *Biosens. Bioelectron.*, 2011, **27**, 46–52.  
21  
22 466 41 M. S. Chiriaco, F. De Feo, E. Primiceri, A. G. Monteduro, G. E. De Benedetto, A.  
23  
24 467 Pennetta, R. Rinaldi and G. Maruccio, *Talanta*, 2015, **142**, 57–63.  
25  
26 468 42 E. Marín-Barroso, C. M. Moreira, G. A. Messina, F. A. Bertolino, M. Alderete, G. J.  
27  
28 469 A. A. Soler-Illia, J. Raba and S. V. Pereira, *Microchem. J.*, 2018, **142**, 78–84.  
29  
30  
31  
32  
33 470  
34  
35  
36  
37  
38  
39  
40  
41  
42  
43  
44  
45  
46  
47  
48  
49  
50  
51  
52  
53  
54  
55  
56  
57  
58  
59  
60

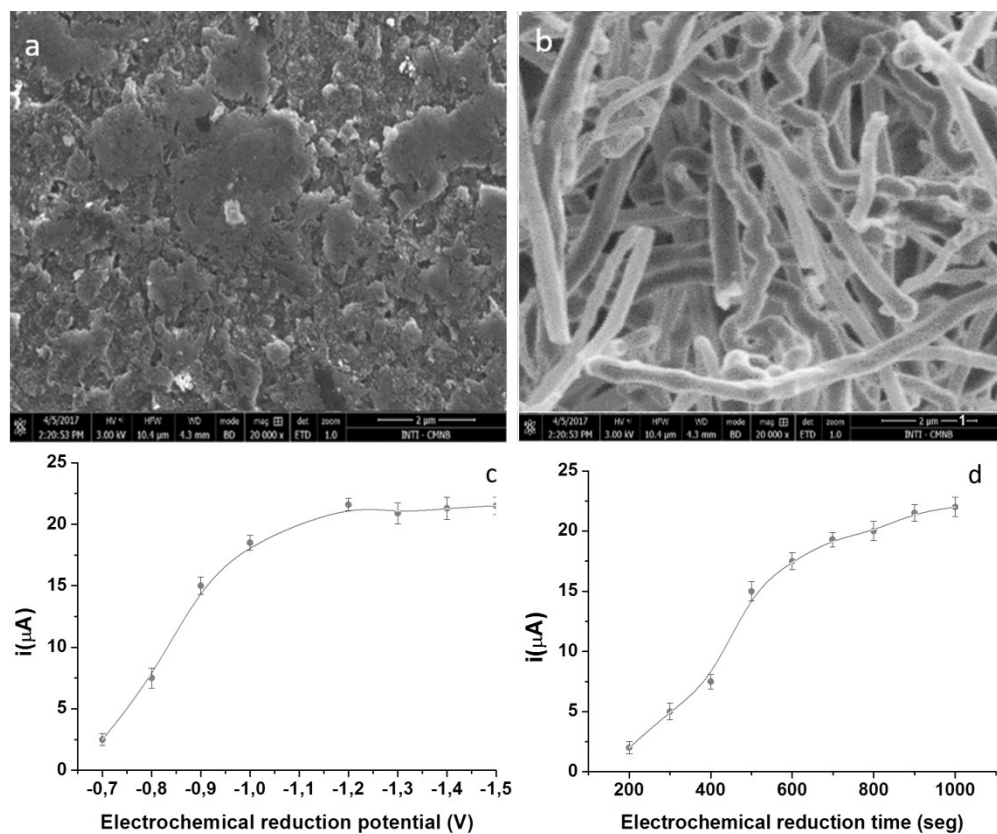


Schematic representation of the electrode modification and gliadin determination procedures.

451x232mm (96 x 96 DPI)

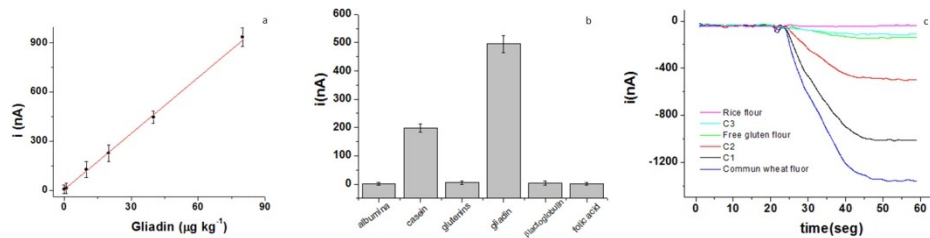


318x232mm (96 x 96 DPI)



(a) Characterization SEM image of unmodified SPCE, (b) SEM image of CNFs / SPCE. (c) Effect of electroreduction potential with the presence of 1 mM  $[\text{Fe}(\text{CN})_6]^{4-/-3-}$  in PBS pH 7.2 and an electroreduction time of 800 s from -0.7 V to -1.5 V (d) Effect of electrochemical reduction time with the presence of 1 mM  $[\text{Fe}(\text{CN})_6]^{4-/-3-}$  in PBS pH 7.2 and an electrochemical reduction potential -1.2 V from 200 s to 1000 s.

548x454mm (96 x 96 DPI)



(a) Calibration curve of the immunosensor using different gliadin standard concentrations Error bar = SD ( $n = 5$ ). (b) The selectivity of the system was evaluated against  $40 \mu\text{g kg}^{-1}$  albumin, casein, glutenin from wheat, gliadin,  $\beta$  lactoglobulin and folic acid, following the procedure described for the electrochemical determination of gliadin content at a potential value of  $-0.15 \text{ V}$  and (c) Amperometric response of the immunosensor to gliadin: Rice flour (pink line), Gluten free flour (green line), Control sample  $5.5 \text{ ppm}$  (light blue line), Control sample  $20 \text{ ppm}$  (red line) Control Sample  $50 \text{ ppm}$  (black line), Common wheat flour (Blue line). Error bar = SD ( $n = 5$ ).

447x120mm (96 x 96 DPI)

Samples no.	Gliadin content mg kg <sup>-1</sup>	Found with spiked gliadin <sup>a</sup> mg kg <sup>-1</sup>	Recovery (%)	CV (%) (n=6)
Manioc flour (2)	Nd	10.21	102.10	4.71
Rice flour (2)	Nd	9.85	98.50	3.80
Gluten free flour (3)	3.01	12.87	98.92	4.93
Common wheat flour (3)	59.06	69.56	100.72	3.98

<sup>a</sup> The data was obtained from six independent experiments (n = 6). The samples were spiked with 10 mg kg<sup>-1</sup> of gliadin.

Nd: Not detected

System	Detection	Sample	LOD **	Ref.
ELISA - Competitive	Spectrometry	Different food samples	2.9 ppm	(33)
(LC-ESI-MS/MS)*	Mass spectrometry	Flours and seeds, pasta, biscuits, cookies	5 ppm	(36)
Aptasensor	Amperometric	Fixamyl, rolled oats, fit Snack	0.113 ppm	(37)
Aptasensor	Impedance	Beer, toasted bread, rice and corn flour	0.05 ppm	(38)
Competitive magneto immunosensor	Optical detection	Beer and skimmed milk	0.0057 ppm	(40)
Immunosensor	Impedance	Beer	0.2 ppm	(41)
Immunosensor	Fluorescence	Beer, flour, and noodles.	0.025 ppm	(42)
Immunosensor	Amperometry	Flour	0.005 ppm	-

\*Liquid chromatography-electrospray ionization-tandem mass spectrometry.

\*\* LOD calculated for food samples taking all dilutions into consideration.

Published on 23 March 2019. Downloaded by University of Edinburgh on 3/25/2019 3:49:12 PM.